

Numerical Results for the System Noise Temperature of an Aperture Array Tile and Comparison with Measurements

M.V. Ivashina ^{*1}, E.E.M. Woestenburg ^{†2}, L. Bakker ^{‡2}, and R.H. Witvers ^{§ 2}

¹Department of Earth and Space Sciences, Chalmers University of Technology, Sweden

²The Netherlands Institute for Radio Astronomy (ASTRON)

October 15, 2011

1 Introduction

This work has been supported in part by the Netherlands Organization for Scientific Research (APERTIF project funded by NWOGroen), the Swedish Agency for Innovation Systems VINNOVA and Chalmers University of Technology (VINNMER - Marie Curie Actions international qualification fellowship). Some results of this work have been recently published in [1, 2].

This report is a shortened version of the original ASTRON report (RP324, 2011) which is publically available upon request. The purpose of this report is to document the noise performance of the Apertif array receiver which has been used to measure its performance as an aperture array and to characterize the recently developed noise measurement facility THACO. The receiver system is the second prototype of APERTIF (DIGESTIF2) [3, 4] that includes the array antenna of 144 dual-polarized TSA elements, 144 Low Noise Amplifiers (LNAs) ($T_{\min} = 35\text{-}40\text{K}$) and the data recording/storing facilities of the initial test station that allow for off-line digital beamforming.

The primary goal of this study is to compare the measured receiver noise temperatures with the simulated values for several practical beamformers, and to predict the associated receiver noise coupling contribution, antenna thermal noise and ground noise pick-up (due to the back radiation). The measurements were performed over a wide frequency band and scan range. In the course of the measurements, the 4, 16, 25 and 49 active antenna elements were used in beamforming, while the remaining elements were connected to the LNAs with the outputs terminated in matched loads. The experimental results were obtained when the receiver with 4- and 16-element analog beamformers was placed inside THACO (a metal shielding cabin which was designed to mitigate the noise contributions due to the ground and trees) and in the open environment at Westerbork near the Westerbork Synthesis Radio Telescope (WSRT), using digital beamforming. The details of these measurements can be found in [2].

Since, the digital data recording-storing facilities are available for the DIGESTIF array receiver, one can also evaluate the system noise temperature for beamforming scenarios that are based on standard signal processing algorithms [5]–[6] and the noise correlation coefficients between the array channels. In this report, we therefore show the range of the realized system noise temperatures when an embedded element only and all

*ivashina@chalmers.se

†woestenburg@astron.nl

‡bakker@astron.nl

§witvers@astron.nl

array elements are used in beamforming. These results demonstrate the *pros* and *cons* of the considered low-gain antenna and high gain digital array receivers for the purpose of the noise temperature characterization in an open environment and inside a shielding cabin such as THACO.

2 The model of the array antenna

The array consists of 2×72 aluminium Tapered Slot Antenna (TSA) elements with a pitch of 11 cm (0.52λ at 1420 MHz) on a rectangular 8×9 grid. Each TSA is fed by a wideband microstrip feed which has been integrated with an LNA on a printed circuit board. This design features a very short transmission line between the antenna and the LNA, since the circular slotline cavity has been moved sideways. More details on the array design and the numerical approach used for the EM-analysis of the antenna can be found in [7] and [6, 8], respectively. The simulations of the antenna have been carried out using CAESAR software that is an array system simulator, developed at ASTRON [9]. Note that these simulations did not take into account the effect of the contributions from obstacles (trees and telescopes/buildings) near the horizon.

3 The noise model of the receiver system

The noise model used in this study is based on the equivalent system representation as described in [10]. According to this representation, the sensitivity of the array receiver can be computed as follows:

$$\frac{A_{eff}}{T_{sys}} = \frac{A_{ph}\eta_{ap}}{T_{ext} + \left(\frac{1 - \eta_{rad}}{\eta_{rad}}\right) T_{amb} + \left(\frac{1}{\eta_{rad}}\right) T_{Eq}^{LNA}}. \quad (1)$$

where A_{ph} and T_{sys} are the physical antenna area and system noise temperature, respectively. The latter consists of three main contributions: (i) The external noise contribution - the ground noise picked up due to antenna back radiation, which was computed from the simulated illumination pattern of the antenna array for the specified beam former weights, (ii) the thermal antenna noise due to the losses in the conductor and dielectric materials of TSAs and microstrip feeds. The conductor losses are computed through the evaluation of the antenna radiation efficiency using the methodology detailed in [11] and the dielectric losses are computed based on the experimental evaluation of the feed loss [12] and (iii) the noise due to LNAs which is dependent upon the noise properties of LNAs and active reflection coefficients seen at the ports of the antenna array. Note, that by using this definition of T_{sys} , all noise temperature contributions are referenced to the sky (in front of the antenna aperture).

It is important to note that the system noise temperature which is calculated from the measured Y-factor is also referenced to the sky. Therefore, to distinguish between the external noise, antenna thermal noise and receiver contributions, one needs to know the beam shape (to compute T_{ext}) and radiation efficiency η_{rad} of the antenna, which are in general dependent on the beamformer weights.

4 The model of the beamformer used to compute the optimal weights

The beamformer model used in this study is based on the mathematical framework which has been described in [6]. Within this framework, the array receiver system is subdivided into two blocks: (i) the front-end including the array antenna, Low Noise Amplifiers (LNAs); and (ii) the beamformer with complex conjugated weights $\{w_n^*\}_{n=1}^N$ and an ideal (noiseless/reflectionless) power combiner realized in software. Here, $\mathbf{w}^H = [w_1^*, \dots, w_N^*]$ is the beamformer weight vector, H is the Hermitian transpose, and the asterisk denotes the complex conjugate. Furthermore, $\mathbf{a} = [a_1, \dots, a_N]^T$ is the vector holding the transmission-line voltage-wave amplitudes at the beamformer input (the N LNAs outputs). Hence, the fictitious beamformer output voltage v (across Z_0) can be written as $v = \mathbf{w}^H \mathbf{a}$, and the receiver output power as $|v|^2 = vv^* =$

$(\mathbf{w}^H \mathbf{a})(\mathbf{w}^H \mathbf{a})^* = (\mathbf{w}^H \mathbf{a})(\mathbf{a}^T \mathbf{w}^*)^* = \mathbf{w}^H \mathbf{a} \mathbf{a}^H \mathbf{w}$, where the proportionality constant has been dropped as this is customary in array signal processing and because we will consider only ratios of powers.

Although each subsystem can be rather complex and contains multiple internal signal/noise sources, it is characterized externally (at its accessible ports) by a scattering matrix in conjunction with a noise- and signal-wave correlation matrix. In this manner, the system analysis and weight optimization becomes a purely linear microwave circuit problem. The sensitivity metric $A_{\text{eff}}/T_{\text{sys}}$, which is the effective area of the antenna system divided by the system equivalent noise temperature, can be expressed in terms of the Signal-to-Noise Ratio (SNR) and the normalized flux density S_{source} of the source (in Jansky, $1 \text{ [Jy]} = 10^{-26} \text{ [Wm}^{-2}\text{Hz}^{-1}\text{]})$ as

$$\frac{A_{\text{eff}}}{T_{\text{sys}}} = \frac{2k_B}{S_{\text{source}}} \text{SNR}, \quad \text{where} \quad \text{SNR} = \frac{\mathbf{w}^H \mathbf{P} \mathbf{w}}{\mathbf{w}^H \mathbf{C} \mathbf{w}}, \quad (2)$$

and where k_B is Boltzmann's constant. The SNR function is defined as a ratio of quadratic forms where \mathbf{C} is a Hermitian spectral noise-wave correlation matrix holding the correlation coefficients between the array receiver channels, i.e., $C_{mk} = \mathbf{E}\{c_m c_k^*\} = \overline{c_m c_k^*}$ (for $k, m = 1 \dots N$). Here, c_m is the complex-valued voltage amplitude of the noise wave emanating from channel m (see [13] and references therein), which includes the external and internal noise contributions inside the frontend block. We consider only a narrow frequency band, and assume that the statistical noise sources are (wide-sense) stationary random processes which exhibit ergodicity, so that the statistical expectation can be replaced by a time average (as also exploited in hardware correlators). \mathbf{C} is nonzero if noise sources are present in the external environment and inside the system, due to e.g. the ground, LNAs, and sky. For a single point source on the sky, the signal-wave correlation matrix $\mathbf{P} = \mathbf{e} \mathbf{e}^H$ is a one-rank positive semidefinite matrix. The vector $\mathbf{e} = [e_1, e_2, \dots, e_N]^T$ holds the signal-wave amplitudes at the receiver outputs and arises due to an externally applied plane electromagnetic wave \mathbf{E}_i .

4.1 Maximum Sensitivity

Maximizing Eq. (2) amounts to solving the largest root of the determinantal equation [5]: $\det(\mathbf{P} - \text{SNR} \mathbf{C}) = 0$ (cf. [14]). Next, the optimum beamformer weight vector $\mathbf{w}_{\text{MaxSNR}}$ is found through solving the corresponding generalized eigenvalue equation $\mathbf{P} \mathbf{w}_{\text{MaxSNR}} = \text{SNR} \mathbf{C} \mathbf{w}_{\text{MaxSNR}}$ for the largest eigenvalue (SNR) as determined in the previous step. The well-known closed-form solution for the point source case, where \mathbf{P} is of rank 1, is given by [14]

$$\mathbf{w}_{\text{MaxSNR}} = \mathbf{C}^{-1} \mathbf{e}, \quad \text{with} \quad \text{SNR} = \mathbf{e}^H \mathbf{w}_{\text{MaxSNR}} \quad (3)$$

where the eigenvector \mathbf{e} corresponds to the largest eigenvalue of \mathbf{P} .

4.2 Maximum output power or the Conjugate Field Matching (CFM) condition

When \mathbf{C} equals the identity matrix \mathbf{I} (thus equal and uncorrelated output noise powers), the receiver output noise power $\mathbf{w}^H \mathbf{C} \mathbf{w} = \mathbf{w}^H \mathbf{w}$ becomes independent of \mathbf{w} in case its 2-norm $\mathbf{w}^H \mathbf{w}$ is a constant value, typically chosen to be unity. With reference to (3), the weight vector that maximizes the received power, and thus realizes a maximum directive gain (and effective area) in the direction of observation, is therefore

$$\mathbf{w}_{\text{CFM}} = \mathbf{e}. \quad (4)$$

These weights optimally satisfy the Conjugate Field Matching (CFM) condition [15, 16, 17].

4.3 Minimum system noise temperature

Similarly, one can develop an expression for computing the beamformer weights for the minimum T_{sys} , that is the case when the source of interest has no contribution and thus independent on the weights. For this

case, the optimal beamformer is described as:

$$\mathbf{w}_{\text{MinTsys}} = \mathbf{C}^{-1} \mathbf{e}_o \quad (5)$$

where $\mathbf{e}_o = \mathbf{1}$.

5 Numerical results for the 144-channel (full-polarization) beamformer

5.1 Simulation details

The simulations were performed with the newly developed numerical tool box for the CAESAR software [8]. This toolbox was initially aimed at the analysis and optimization of the PAF systems, and has been interfaced with GRASP to compute the overall noise wave scattering matrix due to external and internal noise sources as well as the secondary array patterns after the scattering from the dish. For the present study, we have used the pre-processor of this software to determine the optimal beamformer weights (so as to account for the non-uniform noise distribution of the environment) and to evaluate the receiver noise contributions due to internal noise sources according to the model presented in [10] and [11].

5.2 The array beam noise temperature and its contributions

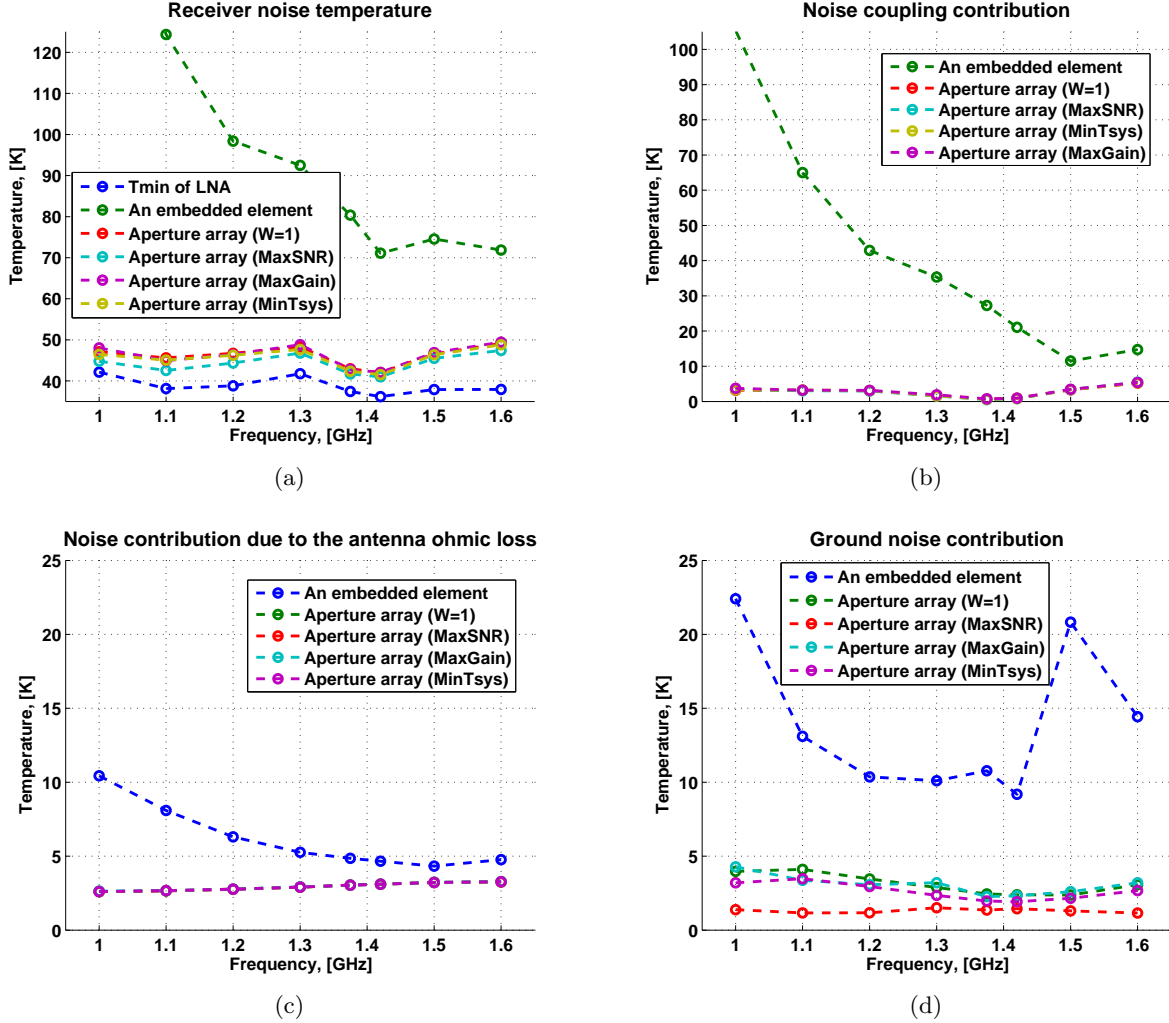


Figure 1: (a) The simulated array beam noise temperature versus frequency and its contributions due to (b) the noise coupling effects in the receiver, (c) the ohmic losses of the antenna and (d) the external noise due to the ground (due to the back radiation of the array, when $\theta \geq 90^\circ$).

6 Results for experimental (bi-scalar) beamformers with 4, 16, 25 and 49 channels

This chapter shows the simulated array antenna properties and compares them with measured receiver noise temperatures versus frequency and scan angle for various beamformer configurations. It starts with a description of the measurement setups and method. It then presents the simulation results for the array antenna patterns and the array beam noise temperatures and its contributions. Finally the results of cross-comparison of the measured Trec at Westerbork and inside THACO are presented.

6.1 Measurement method and setups at Westerbork and inside THACO

For the noise measurements of the APERTIF tile as an aperture array the Y-factor hot/cold method has been used [18]–[19]. During the measurement the tile is placed horizontally on the ground for the measurement in Westerbork (in the open area) or inside the big shielding facility for the Y-factor hot/cold measurements that is called THACO. Two methods were followed, one using analog beam forming with 2x2 and 4x4 elements for the measurements inside THACO, the other using digital beam forming for various beam configurations at the WSRT location. The output signals from the LNAs of a 2x2 and 4x4 array in the centre of the tile inside THACO were added with in-phase combiners, forming broadside beams. The analog output signals of the beam formers were fed to the input of an Agilent Noise Figure Meter 8970B and the noise temperature was determined with the Y-factor method, using the cold sky as a 'cold' load and the roof of THACO, covered with absorbing material, as the 'hot' load. The digital beam forming and processing of the APERTIF prototype system at the WSRT provided a much more flexible system, with which beams could be formed with a larger number of elements, pointing in any desired direction. For the digital processing method, a total of 49 individual antenna elements and LNAs (limited by the number of available receivers at the time of measurements) are connected via 25 m long coaxial cables to the back-end. The back-end electronics is located in a shielded cabin, together with the down converter modules and digital processing hardware [20]. Data are taken with the array facing the (cold) sky as 'cold' load, after which a room temperature absorber is placed over the array for the measurement with the 'hot' load. The data processing takes into account correlations between data from individual elements. The results are stored in a covariance matrix as a function of frequency. Using off-line digital processing, beams with a combination of any of the 49 active elements can be formed and beams may be scanned in any direction by applying weights to the elements of the covariance matrix. In this way the equivalent beam noise temperature as a function of frequency from 1.0 to 1.8 GHz has been determined for 2x2, 4x4, 5x5 and 7x7 element arrays, looking at broadside. Also the equivalent beam noise temperatures as a function of scan angle for the 4x4 and 7x7 element arrays have been determined.

6.2 Simulated antenna beam directivity and noise temperatures

In this section, we present the numerical results for practical beamformers for the frequencies ranging from 1 GHz to 1.6 GHz and over the scan range within which θ changes from 0° to 85° and $\phi = 0 - 360^\circ$. The practical beamformers combine the signals received by 4, 16, 25 and 49 elements. The numerical results include the directivity of the array antenna (see Fig. 2 and the receiver noise temperature and its contributions due to noise coupling effect, antenna ohmic loss, and ground noise due to back radiation (see Fig. 3–??).

Figure 3(a) shows the receiver noise temperatures of the DIGESTIF tile that were computed for the boresight direction of observation at 8 frequency points within the bandwidth of 1-1.6 GHz. These results clearly demonstrate that for all practical beamformers the on-axis beam noise temperature is weakly dependent on frequency and takes values between 42 and 61 K that are 5-30% higher than the minimum noise temperature of LNAs ($T_{\min} = 35 - 40$)K. The noise contributions due to the receiver noise coupling effects T_{coup} , antenna ohmic losses T_{rad} and external (ground) noise pick-up T_{ext} , as shown on fig. 3(b), 3(c) and 3(d) do not exceed 13, 3.5 and 6.5 K, respectively. At 1.42 GHz - the frequency at which the array design was optimized - the temperatures T_{coup} and T_{ext} and the total receiver temperature take the minimum values within the operational bandwidth as the result of the minimized impedance mismatch loss and relatively low side and back radiation levels. Figure 4(a)-(d) shows how the receiver noise and its weight-dependent noise components vary with scan angle for beamformers with 16 and 49 elements at 1 GHz and 1.42 GHz. For these beamformers, respectively, the increase of the noise temperatures is less than 20% when the scan angle is smaller than $\sim 30^\circ$ and $\sim 40^\circ$ off boresight direction. For larger scan angles, however, T_{rec} rapidly increases and becomes as high as 80-160 K depending on the number of active antenna elements, scan plane and frequency. Such high values are mainly due to the strong mutual coupling between antenna elements at low frequencies (causing the rise of the receiver noise coupling contribution as observed on fig. 5(c)) and high side-lobe levels at high frequencies for scanned beams.

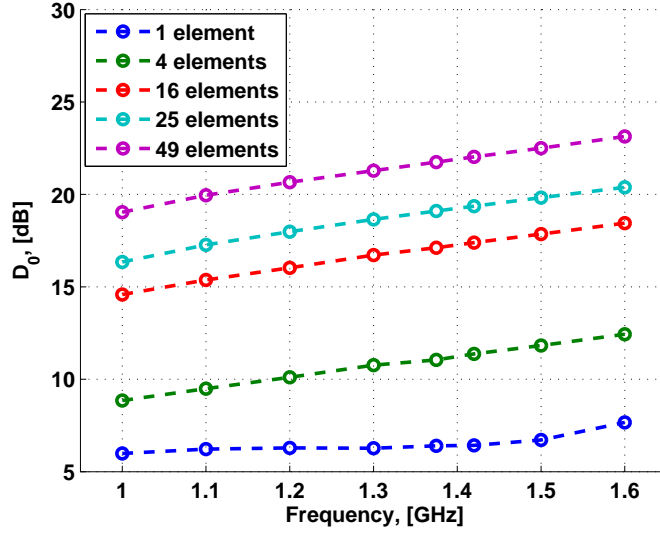


Figure 2: The array directivity versus frequency.

6.3 Comparison with measurements in the open environment at Westerbork

This subsection compares the predicted and measured receiver noise temperatures versus frequency. The results of cross-comparison of the measured T_{rec} at Westerbork (in the open environment) and inside THACO (which is expected to shield the receiver from the ground noise) are presented. Also, the measured and modeled noise temperatures of a single Vivaldi element receiver inside THACO are shown.

Upon collecting the simulation and measurement results, we can compute the relative difference between the modeled and measured receiver noise temperatures. Figures 6-7 show both the simulated and measured T_{rec} as well as their relative difference as a function of frequency and scan angle. As one can see on fig.6(c), the relative difference between simulations and measurements is smaller than 20% over the entire frequency range for all practical beamformers, except for the beamformer with 4 active channels in the region of 1-1.2 GHz. At these frequencies the 4-element subarray has a rather low gain (<10 dB) and, thus the experimental receiver picks up the noise due to the buildings and trees that are present in the actual environment, but were not accounted for in the model. This reasoning is supported by the measurements which were done inside the shielding cabin (THACO) (see fig.8(c)). For the latter tests, the measured noise temperatures for the 4-channel beamformer lie within the region of the simulated values with 15-20% difference at most frequencies.

The agreement between the simulated and measured noise temperatures over the scan range is also good, and for the beamformers with 16 and 49 channels was found to be at the level of $<25\%$ within the scan range of $\pm(40 - 45^\circ)$. For larger off-axis angles, the measured temperatures are much higher with the difference up to 50% relatively to the corresponding simulated values.

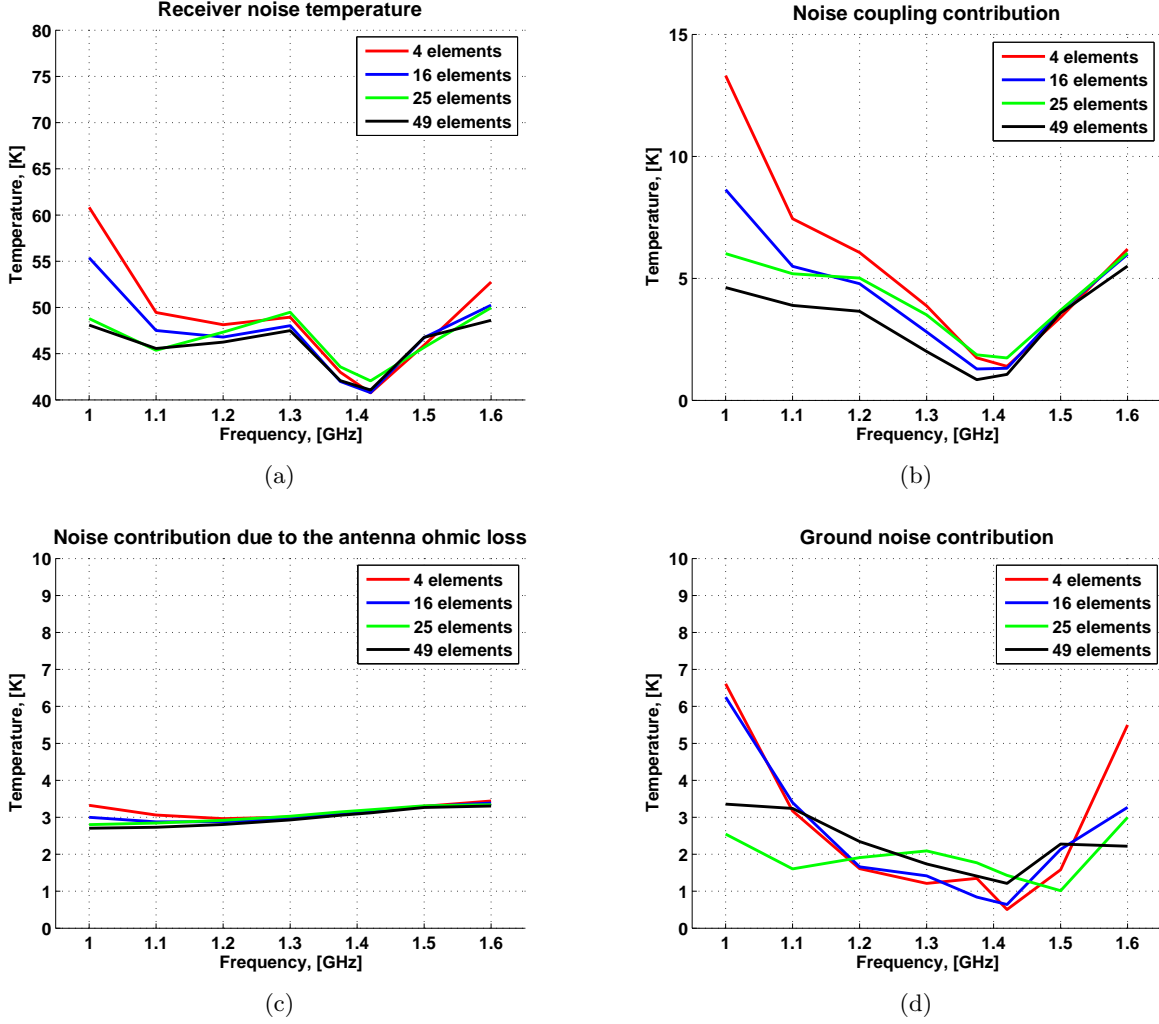


Figure 3: (a) The simulated receiver noise temperature versus frequency and its contributions due to (b) the noise coupling effects in the receiver, (c) the ohmic losses of the antenna and (d) the external noise due to the ground (due to the back radiation of the array, when $\theta \geq 90^\circ$). All temperatures are for broad side beams.

6.4 Comparison with measurements inside THACO

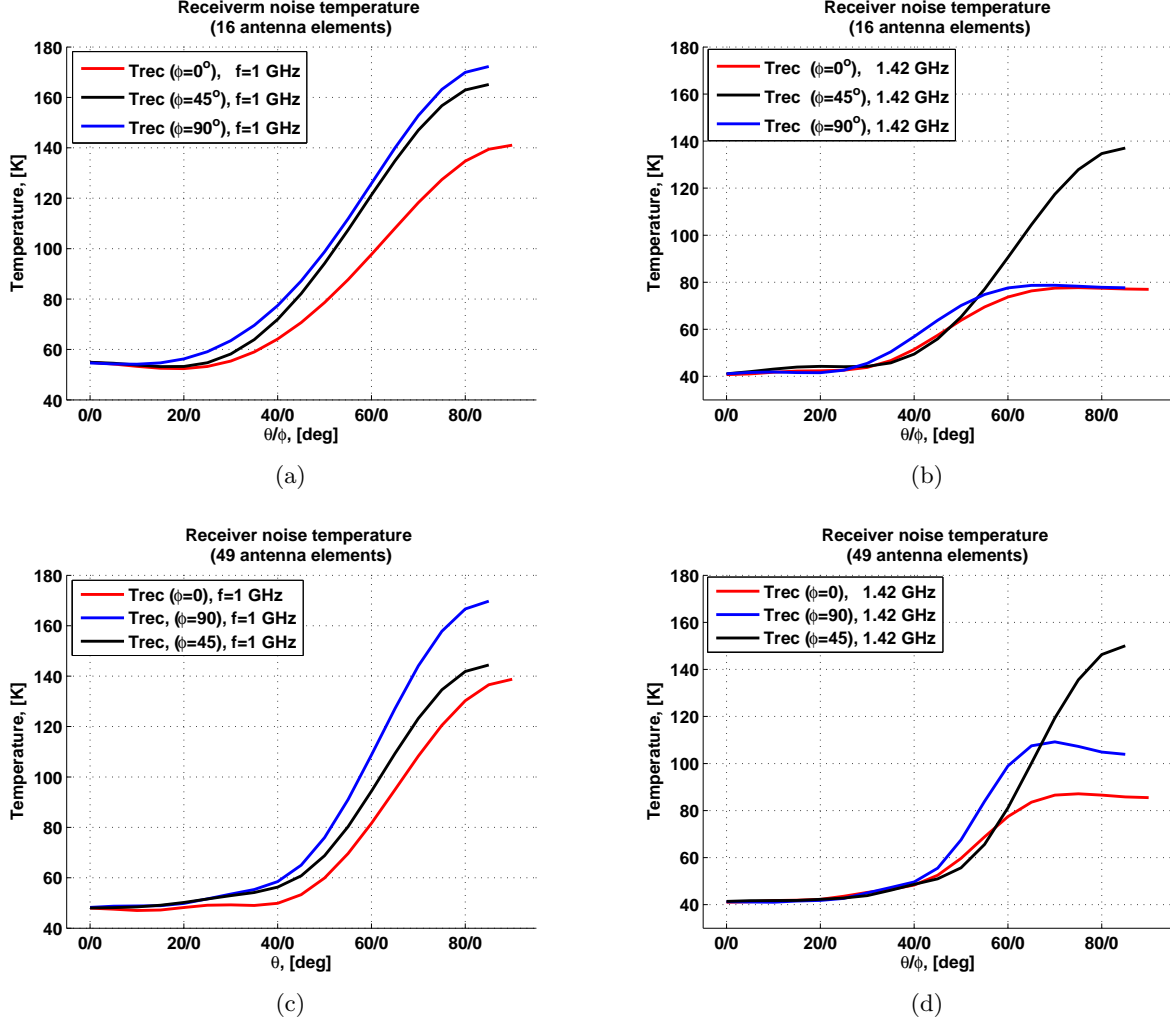


Figure 4: The simulated receiver noise temperatures versus scan angle in three scan planes for beamformers with (a,b) 16 and (c,d) 49 active antenna elements at 1.0 GHz and 1.42 GHz.

7 Conclusions

The noise performance of the aperture array tile receiver has been simulated and compared to the experimental results as obtained through the ‘hot-cold’ measurement procedure inside a shielding cabin (THACO) and in the open environment near WSRT. The measurements have been carried out for several practical beamformers (with 4, 16, 25 and 49 active channels) over the frequency band from 1 to 1.6 GHz and a wide 3D beam scan range. The presented numerical results include the antenna patterns and system noise temperatures T_{sys} for all considered practical situations, as well as separate noise contributions due to the receiver noise coupling effects T_{coup} , antenna ohmic loss T_{rad} and external (sky and ground) noise T_{ext} .

The numerical results demonstrate that the on-axis beam noise temperatures take values ranging between 42 and 61 K within the frequency bandwidth and are maximum 30% higher than the minimum noise temperature of LNAs ($T_{min} = 35 - 40$) K. The noise contributions T_{coup} , T_{rad} and T_{ext} do not exceed 13, 3.5 and 6.5 K, respectively for broad side beams. At 1.42 GHz - the frequency at which the antenna was optimized - T_{sys} is lowest, as the result of the minimized impedance mismatch loss and relatively low side and back radiation levels.

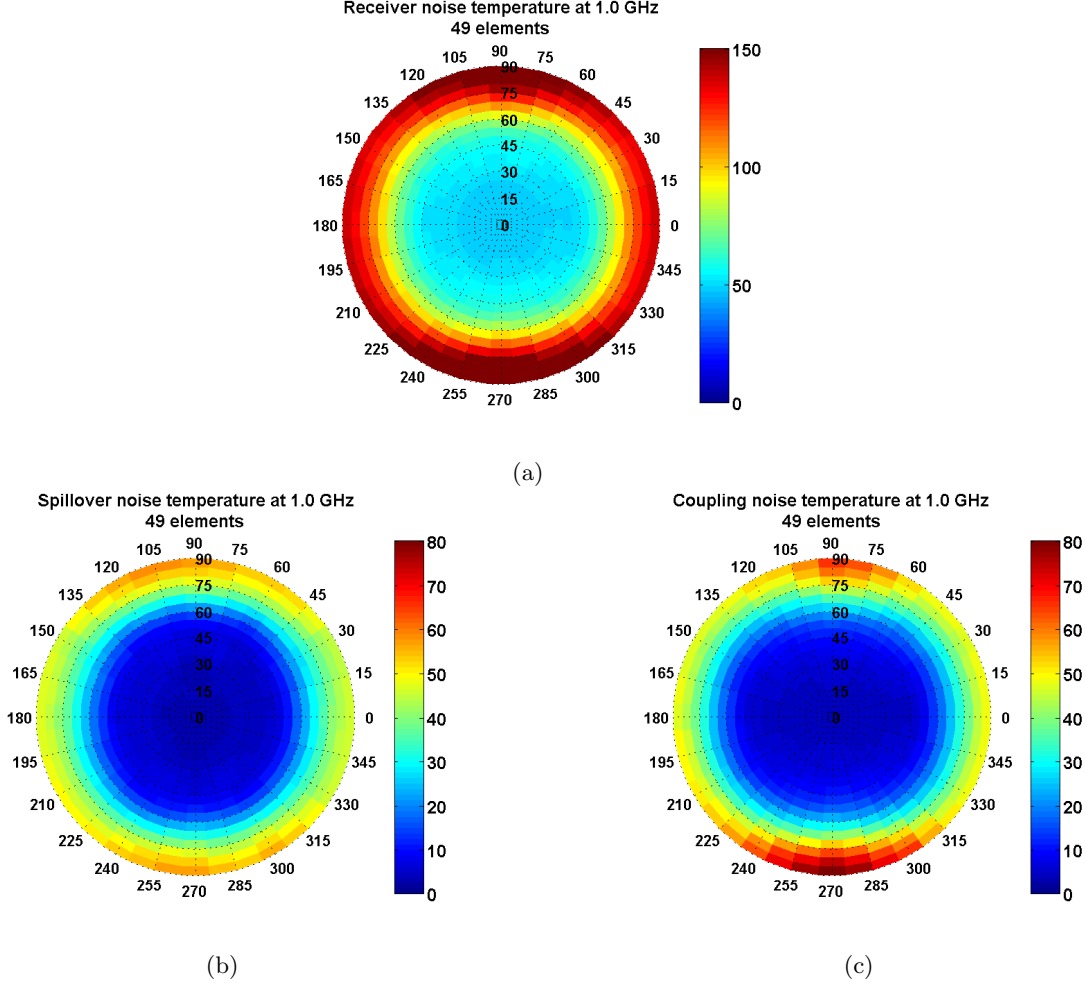


Figure 5: (a) The simulated receiver noise temperature ([K]) over scan angle at 1.0 GHz and its contributions due to (b) the noise coupling effects in the receiver, (c) the ohmic losses of the antenna and (d) the external noise due to the ground (due to the back radiation of the array, when $\theta \geq 90^\circ$).

The receiver noise temperature exhibits a strong dependence on the beamformer weights and degrades when scanning far off boresight direction. For beamformers with 16 and 49 channels respectively, the relative increase of T_{rec} was found to be less than 20% for the scan angles smaller than $\sim 30^\circ$ and $\sim 40^\circ$, and a factor 2-4 for larger angles, depending on frequency and beamformer. Such high values of T_{rec} are mainly due to the strong mutual coupling between antenna elements at low frequencies (causing the rise of T_{coup} and high side-lobe levels at high frequencies for scanned beams).

There is a good agreement between simulations and measurements that were performed in the open environment at Westerbork. The relative difference between the modeled and measured T_{sys} is smaller than 20-25% over the entire frequency band and within the scan range of $\pm(40 - 45^\circ)$, except for the 4-channel beamformer for which this difference can be twice as large. For the latter beamformer case, the antenna pattern is rather broad (the gain is <10 dB) and, thus the experimental receiver can pick up an additional noise component due to the buildings and trees that are present in the actual environment, but were not accounted for in the model. This reasoning is supported by the measurements inside the shielding cabin (THACO) for which the agreement with simulations significantly improves. Furthermore, for large off boresight scan angles, the temperatures as measured in the open environment are much higher than the

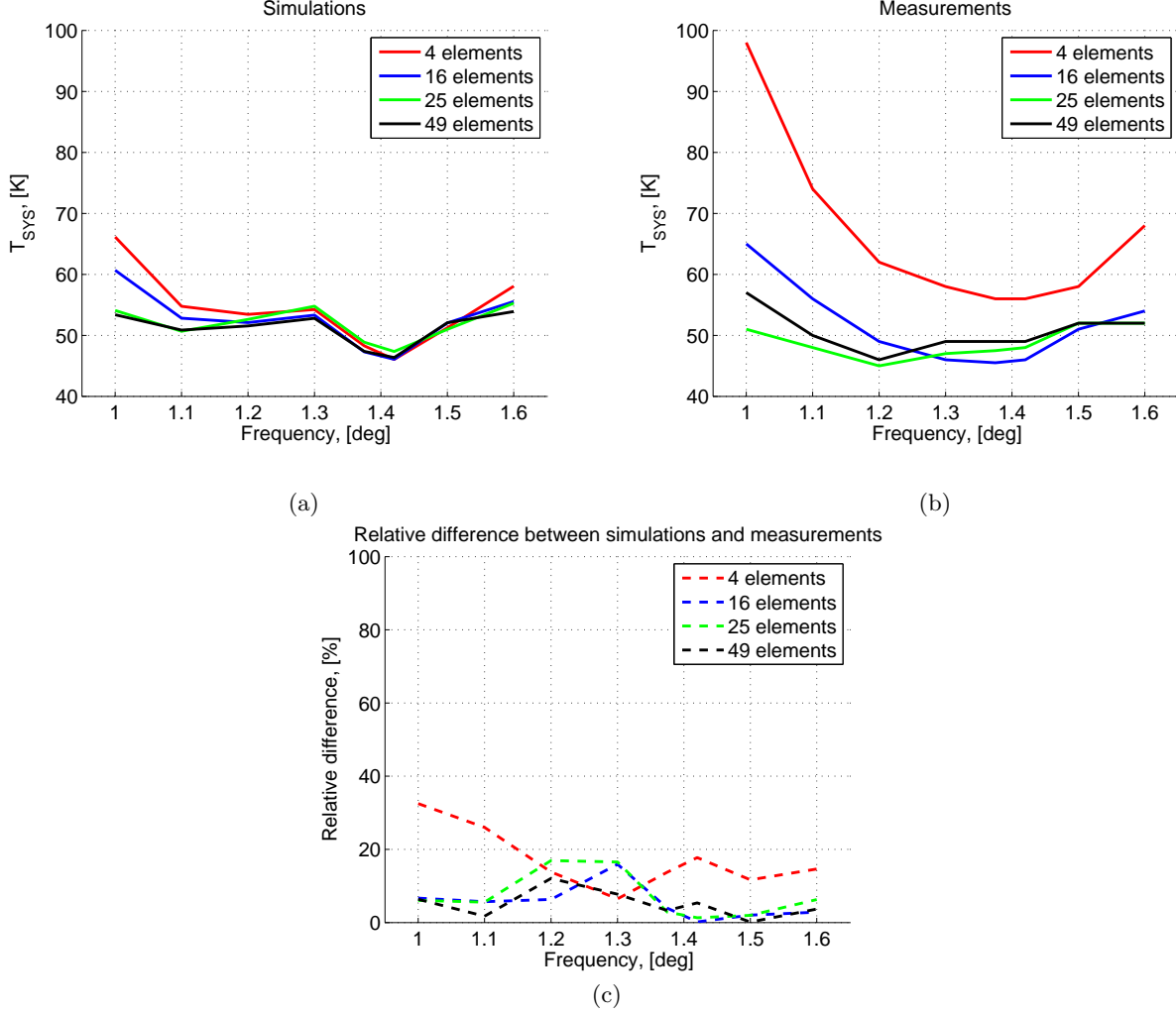


Figure 6: (a) The simulated and (b) measured system noise temperatures ($T_{\text{SYS}} = T_{\text{rec}} + T_{\text{sky}}$) versus frequency and (c) the relative difference between them.

simulated ones, most likely due to the above mentioned effects of the noisy environment of which the exact temperature distribution is not well known.

8 Acknowledgements

This work has been supported in part by the Netherlands Organization for Scientific Research (APER-TIF project funded by NWO Groot), the Swedish Agency for Innovation Systems VINNOVA and Chalmers University of Technology (VINNMER - Marie Curie Actions international qualification fellowship).

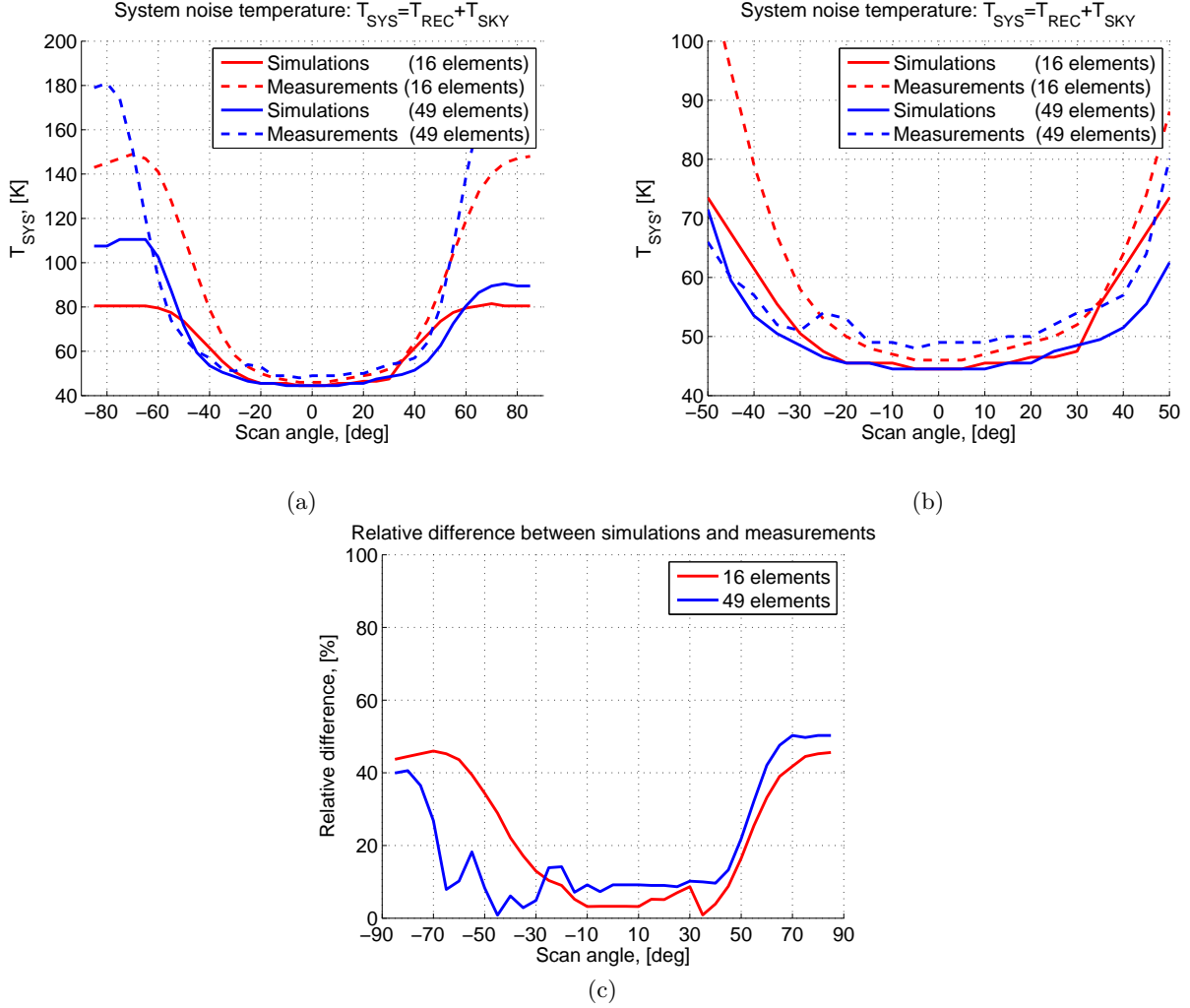


Figure 7: The simulated and measured receiver noise temperatures versus scan angle for (a) a large and (b) small scan range and (c) the relative difference between them.

References

- [1] E. E. M. Woestenburger, L. Bakker, M. Ruiter, M. V. Ivashina, and R. H. Witvers, "Thaco, a test facility for characterizing the noise performance of active antenna arrays," in *Proc. of European Microwave Week (EuMW2011)*, Manchester, UK, Oct 9-14, 2011.
- [2] E. E. M. Woestenburger, L. Bakker, and M. V. Ivashina, "Experimental results for the sensitivity of a low noise aperture array tile," *accepted to IEEE Trans. Antennas Propagat.*, 2011.
- [3] M. Verheijen, M. A. W. Oosterloo, L. Bakker, M. Ivashina, and J. van der Hulst, "Apertif, a focal plane array for the wsrt," in *The Evolution of Galaxies through the Neutral Hydrogen Window*, Arecibo Observatory, Puerto Rico, Feb 1-3, 2008. [Online]. Available: <http://arXiv.org:0806.0234>
- [4] W. A. van Cappellen, L. Bakker, and T. A. Oosterloo, "Experimental results of a 112 element phased array feed for the westerbork synthesis radio telescope," in *Proc. IEEE AP-S International Symposium*, Charleston, USA, June 2009, pp. 1522–3965.

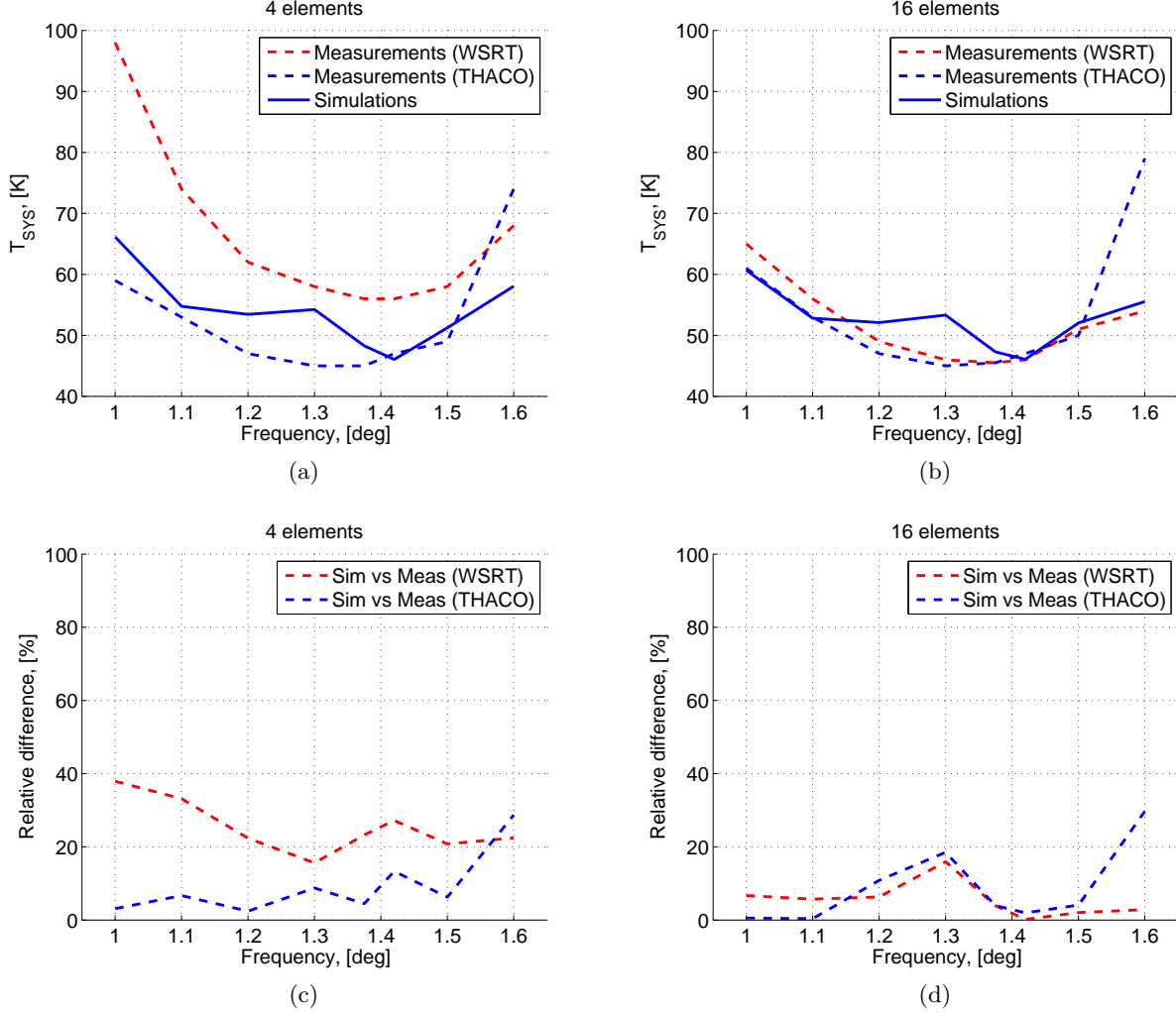


Figure 8: The simulated and measured receiver noise temperatures versus frequency for (a) 4-element and (b) 16-element beamformers and (c,d) the relative difference between the measurements and simulations for the corresponding beamformers.

- [5] H. L. van Trees, *Optimum Array Processing*. New York: John Wiley and Sons, Inc., 2002.
- [6] M. V. Ivashina, O. Iupikov, R. Maaskant, W. A. van Cappellen, and T. Oosterloo, “An optimal beamforming strategy for wide-field surveys with phased-array-fed reflector antennas,” *IEEE Trans. Antennas Propag.*, vol. 59, no. 6, pp. 1864–1875, June 2011.
- [7] M. Arts, M. Ivashina, O. Iupikov, L. Bakker, and R. van den Brink, “Design of a low-loss low-noise tapered slot phased array feed for reflector antennas,” in *Proc. European Conference on Antennas and Propag. (EuCAP)*, Barcelona, Spain, Apr. 2010.
- [8] M. Ivashina, O. Iupikov, and W. van Cappellen, “Extending the capabilities of the grasp and caesar software to analyze and optimize active beamforming array feeds for reflector systems,” in *Proc. Int. Conf. on Electromagn. in Adv. Applicat. (ICEAA)*, Sydney, Sept. 2010, pp. 197–200.

- [9] R. Maaskant and B. Yang, "A combined electromagnetic and microwave antenna system simulator for radio astronomy," in *Proc. European Conference on Antennas and Propag. (EuCAP)*, Nice, France, Nov. 2006, pp. 1–4.
- [10] M. V. Ivashina, R. Maaskant, and B. Woestenburger, "Equivalent system representation to model the beam sensitivity of receiving antenna arrays," *IEEE Antennas Wireless Propag. Lett.*, vol. 7, no. 1, pp. 733–737, 2008.
- [11] R. Maaskant, D. J. Bekers, M. J. Arts, W. A. van Cappellen, and M. V. Ivashina, "Evaluation of the radiation efficiency and the noise temperature of low-loss antennas," *IEEE Antennas Wireless Propag. Lett.*, vol. 8, no. 1, pp. 1166–1170, Dec. 2009.
- [12] M. V. Ivashina, E. A. Redkina, and R. Maaskant, "An accurate model of a wide-band microstrip feed for slot antenna arrays," in *Proc. IEEE AP-S International Symposium*, Hawaii, USA, June 2007, pp. 1953–1956.
- [13] S. W. Wedge and D. B. Rutledge, "Wave techniques for noise modeling and measurement," *IEEE Trans. Antennas Propag.*, vol. 40, no. 11, pp. 2004–2012, Nov. 1992.
- [14] D. K. Cheng and F. I. Tseng, "Maximisation of directive gain for circular and elliptical arrays," *Proc. Inst. Elec. Eng.*, pp. 589–594, May 1967.
- [15] M. V. Ivashina, M. Ng Mou Kehn, and P.-S. Kildal, "Optimal number of elements and element spacing of wide-band focal plane arrays for a new generation radio telescope," in *Proc. European Conference on Antennas and Propag. (EuCAP)*, Edinburg, UK, Nov. 2007, pp. 1–4.
- [16] M. V. Ivashina, M. Kehn, P.-S. Kildal, and R. Maaskant, "Decoupling efficiency of a wideband vivaldi focal plane array feeding a reflector antenna," *IEEE Trans. Antennas Propag.*, vol. 57, no. 2, pp. 373–382, Feb. 2009.
- [17] P. J. Wood, *Reflector antenna analysis and design*. Stevenage, U.K., and New York: IEE, Peter Peregrinus LTD., 1980.
- [18] E. E. M. Woestenburger and K. F. Dijkstra, "Noise characterization of a phased array tile," in *Proc. European Microwave Conference*, Germany, 2003.
- [19] K. F. Warnick, B. D. Jeffs, J. Landon, J. Waldron, R. Fisher, and R. Norrod, "Byu/nrao 19-element phased array feed modeling and experimental results," in *Proc. URSI General Assembly*, Chicago, 2007.
- [20] W. A. van Cappellen and L. Bakker, "Apertif: Phased array feeds for the westerbork synthesis radio telescope," in *IEEE Int. Symp. on Phased Array Systems and Technology*, Boston, 2010.